Clinical Science (2017) **131**, 285–296 doi: 10.1042/CS20160469

Original Paper

Defective adaptive thermogenesis contributes to metabolic syndrome and liver steatosis in obese mice

Laurence Poekes*, Vanessa Legry*, Olivier Schakman†, Christine Detrembleur‡, Anne Bol§, Yves Horsmans‖, Geoffrey C. Farrell¶ and Isabelle A. Leclercq*

*Laboratory of Hepato-Gastroenterology, Institut de Recherche Expérimentale et Clinique, Université catholique de Louvain, 1200 Brussels, Belgium
†Laboratory of Cellular Physiology, Institute of NeuroScience, Université catholique de Louvain, 1200 Brussels, Belgium
‡Computer Assisted and Robotic Surgery, Institut de Recherche Expérimentale et Clinique, Université catholique de Louvain, 1200 Brussels, Belgium
§Molecular Imaging, Radiotherapy and Oncology Unit, Université catholique de Louvain, 1200 Brussels, Belgium
‖Gastroenterology Unit, Cliniques Universitaires Saint-Luc, Université Catholique de Louvain, 1200 Brussels, Belgium
¶Liver Research Group, Australian National University Medical School, The Canberra Hospital, 2605 Canberra, ACT, Australia

Abstract

Fatty liver diseases are complications of the metabolic syndrome associated with obesity, insulin resistance and low grade inflammation. Our aim was to uncover mechanisms contributing to hepatic complications in this setting. We used *foz/foz* mice prone to obesity, insulin resistance and progressive fibrosing non-alcoholic steatohepatitis (NASH). *Foz/foz* mice are hyperphagic but wild-type (WT)-matched calorie intake failed to protect against obesity, adipose inflammation and glucose intolerance. Obese *foz/foz* mice had similar physical activity level but reduced energy expenditure. Thermogenic adaptation to high-fat diet (HFD) or to cold exposure was severely impaired in *foz/foz* mice compared with HFD-fed WT littermates due to lower sympathetic tone in their brown adipose tissue (BAT). Intermittent cold exposure (ICE) restored BAT function and thereby improved glucose tolerance, decreased fat mass and liver steatosis. We conclude that failure of BAT adaptation drives the metabolic complications of obesity in *foz/foz* mice, including development of liver steatosis. Induction of endogenous BAT function had a significant therapeutic impact on obesity, glucose tolerance and liver complications and is a potential new avenue for therapy of non-alcoholic fatty liver disease (NAFLD).

Key words: brown adipose tissue, energy expenditure, metabolic syndrome, non-alcoholic fatty liver disease, obesity, thermogenesis.

INTRODUCTION

Obesity is a major public health issue worldwide, and recent studies report an increasing prevalence of overweight and obesity in the last decades [1,2]. Obesity associates with systemic metabolic and inflammatory alterations (defined as the metabolic syndrome) and increased risk for Type 2 diabetes, cardiovascular diseases and non-alcoholic fatty liver disease (NAFLD) and its progressive form, non-alcoholic steatohepatitis (NASH). In most instances, predisposition to obesity is multifactorial and polygenic but energy imbalance with more calories consumed than expended is an omnipresent feature [3]. The energy in excess is stored as lipids, in adipose tissue in the first line, and eventually in other organs such as the liver. Increased energy substrate utilization by physical activity and/or decreased food intake by dietary therapy or bariatric surgery have positive impact on body weight (BW) and metabolic complications [4]. In patients with NAFLD, a 5% weight loss has been shown to be effective in reducing insulin resistance, decreasing plasmatic transaminases [5] and improving liver steatosis [6]. The everyday experience shows nonetheless that lifestyle interventions are poorly sustainable in the long run calling for additional therapeutic intervention.

Non-shivering thermogenesis increases energy expenditure [7]. The brown adipose tissue (BAT) is the main thermogenic tissue and, unlike white adipose tissue (WAT) devoted to fat storage, possesses the capacity to convert energy substrates such as glucose and fatty acids into heat through a process controlled by the sympathetic nervous system [8]. BAT thermogenesis is primarily

Abbreviations: ACOX, acyl CoA oxidase; ALMS, Alström syndrome protein 1; α-MT, α-methyl-p-tyrosine; βAR, β adrenergic receptor; AUC, area under the curve; BAT, brown adipose tissue; BMP8B, bone morphogenetic protein 8B; BW, body weight; COX-II, cytochrome c oxidase subunit 2; DIO2, type II iodothyronine deiodinase; epiAT, epididymal adipose tissue; ^{18}F-FDG, ^{18}F-fluorodeoxyglucose; PET/CT, positron emission tomography–computed tomography; HFD, high-fat diet; ICE, intermittent cold exposure; ingWAT, inguinal white adipose tissue; ip, intraperitoneal; ipGTT, intraperitoneal glucose tolerance test; NAFLD, non-alcoholic fatty liver disease; NASH, non-alcoholic steatohepatitis; ND, normal diet; NE, noradrenaline; OGTT, oral glucose tolerance test; PGC1α, peroxisome proliferator-activated receptor γ co-activator 1 α; PPARα, peroxisome proliferator-activated receptor α; PRDM16, PR domain containing 16; RT-qPCR, real-time quantitative PCR; T3, triiodothyronine; TBX1, T-Box 1; TMEM26, transmembrane protein 26; TNFα, tumour necrosis factor α; UCP1, uncoupling protein-1; WAT, white adipose tissue; WT, wild-type.

Correspondence: Isabelle A. Leclercq (email isabelle.leclercq@uclouvain.be).

involved in the homoeostatic maintenance of body temperature. However, more and more animal and human data support a role for BAT thermogenesis in energy homoeostasis and control of body weight gain. Thus, mice without BAT become obese [9] and, in small series, BAT activity negatively correlates with fat mass and body mass index in humans [10].

In the present study, we investigated mechanisms responsible for rapid progression of obesity and metabolic disturbances in *foz/foz* mice. Of interest, unlike many other animal models of obesity, such as dietary models or leptin deficient *ob/ob* mice that associate with simple steatosis [11], high-fat diet (HFD)-fed *foz/foz* mice develop hepatic complication progressing with time to severe fibrosing NASH [12–15]. The *foz/foz* strain has been selected for a spontaneous mutation in a gene encoding the Alström syndrome protein 1 (ALMS1) of yet unknown function. In humans, mutation in *Alms1* gene leads to Alström syndrome characterized (among others) by early onset diabetes, obesity, NASH and multiple other comorbidities [16]. A previous study associated the obese phenotype of *foz/foz* mice with defective hypothalamic appetite regulation [17] causing hyperphagia. We found here, using a pair-feeding experiment that increased caloric intake is only partly involved as obesity and glucose intolerance were maintained under conditions of caloric restriction. By contrast, we identified defective adaptation of thermogenesis to HFD and to cold exposure as a contributing process to metabolic overload and comorbidities in *foz/foz* mice.

MATERIALS AND METHODS

Animals and diets

The fatty aussie mouse (*foz/foz* mouse) strain on an NOD. B10 background was bred and maintained at a constant temperature of 22 °C unless specified otherwise, and exposed at all times to a 12-h light/12-h dark cycle. Heterozygous mice (foz/+) were used for breeding and homozygous *foz/foz* and wild-type (WT) +/+ male offspring from the same litters for the dietary experiments. The animals were handled according to the guidelines for humane care for laboratory animals established by the Université catholique de Louvain in accordance with European regulations, and the study protocol was approved by the university ethics committee (2012/UCL/MD/026). At 5 weeks of age, mice were switched to a HFD (60% of calories from fat, 0.03% cholesterol-Research Diets D12492) or maintained on normal diet (ND) (standard rodent chow; 10% of calories from fat; Carfil Quality) provided *ad libitum*, hereafter referred to as HFD and ND respectively.

For the pair-feeding experiment, *foz/foz* and WT mice were weaned into individual cages and matched for body weight. *foz/foz* mice were strictly allowed the same amount of HFD consumed *ad libitum* the day before by matched WT counterparts. Mice were either fed *ad libitum* or pair-fed for up to 4 weeks, unless stated otherwise. Food consumption was measured daily at 17:00 hours, and mouse body weight recorded every second day.

At the time of killing, blood was withdrawn by cardiac puncture and organs (liver, epididymal, inguinal and interscapular BATs) dissected, weighted, snap frozen in liquid nitrogen and stored at −80 °C until analyses or fixed in 4% formalin for histological analyses.

Dynamic insulin sensitivity and glucose tolerance tests

Insulin (1 mUI/g body weight, ip) or glucose [1.25 mg/kg body weight ip – intraperitoneal glucose tolerance test (ipGTT)- or 0.063 mg/mouse by oral gavage – oral glucose tolerance test (OGTT)] was administered to 4-h fasted animals and glucose levels monitored on tail blood at 0, 15, 30, 60, 90, 120 and 180 min after the injection using a glucometer (Accuchek). Cumulative area under the curve (AUC) for blood glucose over 180 min was calculated.

Assessment of physical activity

Five-week-old *foz/foz* and WT mice were placed in individual metabolic cages (Bioseb) and fed a ND. After 24 h of acclimatization, spontaneous rearing and locomotor activities were recorded for 48 h as described previously [18]. Then, diet was changed from a ND to a HFD and movements recorded for an additional 48 h. A third recoding was performed after 4 weeks of HFD feeding.

Oxygen consumption

Oxygen consumption was measured in a metabolism chamber, maintained at room temperature (22 °C) or at 7 °C by circulating water. Mice are placed in a removable cage sealed in a cylindrical plastic chamber. CO_2 exhaled by the mouse is absorbed by H_2O-saturated soda lime (Medisorb), so variations in internal pressure are directly proportional to O_2 consumption. Practically, we recorded the volume of air injected to the system (ml/5 min) to balance the pressure and calculate O_2 consumption. Oxygen consumption was normalized by metabolic body weight ($BW^{0.66}$) and values were expressed as $ml \cdot kg^{-0.66} \cdot min^{-1}$ [19].

Thermogenic response to cold exposure

Acute cold exposure

HFD-fed WT and *foz/foz* mice were housed at 30 °C in a vented animal cabinet. After 4 weeks, WT and *foz/foz* mice were transferred to cages (two mice per cage) with no bedding and maintained at 4 °C for 6 h. Body temperature was measured every 2 h using an electronic thermistor equipped with a rectal probe (Bioseb thermometer TK 8851). At the end of the experiment, mice were killed at 4 °C.

Intermittent cold exposure (ICE)

Control mice were kept at 22 °C and tested WT and *foz/foz* mice (two mice per cage), matched for genotype, BW and glycaemia, were exposed to 4 °C ambient temperature for two consecutive hours then returned to the animal house (22 °C) 5 days per week for 4 weeks. On the last day of the experiment, the mice were killed after 6 hours at 4 °C.

PET/CT imaging

^{18}F-fluorodeoxyglucose (150 μCi) (^{18}F-FDG; Betaplus Pharma) was injected into the peritoneal cavity and positron emission tomography-computed tomography (PET/CT) images acquired

1 h later using a Gemini PET/CT system (Philips Healthcare) on anesthetized mice. The PET and CT images were then analysed with the PMod Software. The interscapular BAT was manually delineated in 3D. ^{18}F-FDG BAT uptake was expressed at the percentage of the injected dose per gram of BAT.

Histology, immunohistochemistry (IHC) and immunofluorescence

Five micrometres thick paraffin sections were stained with haematoxylin/eosin. Size of adipocytes and lipid vacuoles were quantified using Visiopharm software. Uncoupling protein-1 (UCP1) was detected by immunohistochemistry using a primary polyclonal rabbit anti-mouse UCP1 Ab (Abcam) and an anti-rabbit streptavidin horseradish-peroxidase-conjugated Ab (EnVision; Dako). Peroxidase activity was revealed with diaminobenzidine (DAB). Tyrosine hydroxylase was visualized by immunofluorescence using anti-tyrosine hydroxylase primary antibody (Abcam) and secondary Alexa Fluor-488 (Thermo Fisher), and quantified using imageJ (three pictures per animal).

TEM

Interscapular BAT was fixed overnight with 2% glutaraldehyde/2% paraformaldehyde in 0.1 M phosphate buffer (pH 7.4) and postfixed for 1 h with 1% OsO_4 in H_2O. Samples were dehydrated and embedded in 75/25 resin/propylene oxide. Ultrathin sections were contrasted with uranyl acetate/lead citrate. For each animal ($n = 2$–3 per group), 10 areas were randomly selected to measure brown adipocyte area and the number of mitochondria per brown adipocyte.

Biochemical analyses

We measured by ELISA plasma C-peptide concentration (Alpco Diagnostics), free triiodothyronine (T3, mybiosource) in BAT homogenized in PBS and cAMP (Enzo Life science), noradrenaline (NE), adrenaline (epinephrine) and dopamine (3-CAT research ELISA, Labor diagnostika nord) in the supernatant of BAT homogenized in 0.01 M HCl and 1 mM EDTA at 0 °C.

NE turnover

We assessed NE turnover by measuring the disappearance rate of NE in the BAT after α-Methyl-p-tyrosine (α-MT) injection, an inhibitor of tyrosine hydroxylase, the rate-limiting enzyme in catecholamine biosynthesis [20]. Mice were killed by cervical dislocation 0 and 1.5 h after α-MT injection (300 mg/kg, ip), and the BAT was rapidly removed to quantify NE content. The log NE concentration was plotted against the time after α-MT administration. The fractional turnover rate (k) was calculated from the slope of the line by linear regression.

RNA, real-time quantitative PCR and mtDNA quantification

cDNA was synthesized from 1 μg RNA. Gene expression was assessed by real-time quantitative PCR with the Step One Plus device and software (Applied Biosystems) using SYBR Green (Applied Biosystems) and gene-specific primers (see Supplementary Table S2). mRNA levels were normalized to that of ribosomal protein L19 (RPL19) as a reference gene.

Total DNA was extracted from BAT using the DNeasy Blood & Tissue Kit (Qiagen). The mtDNA content was inferred by relative DNA abundance of mitochondrial cytochrom c oxidase subunit 2 (*COXII*) gene to that of nuclear β-2-microglobulin assessed by quantitative PCR.

Statistics

All data are presented as mean $\pm$ S.E.M. Statistical analyses were performed using a two-tailed Student t test, a one-way or two-way ANOVA followed by Bonferroni's post-hoc or a two-way ANOVA for repeated measures as appropriate using Graph Pad Prism 5 software. Differences were considered significant at values of $P < 0.05$.

RESULTS

HFD-fed *foz/foz* mice have a severe dysmetabolic phenotype

foz/foz and WT mice have similar body weight at weaning (Supplementary Table S1). During HFD *ad libitum* for 4 weeks, *foz/foz* mice consume more food than WT mice and unlike WT littermates, they become obese with a pronounced increase in adiposity and enlarged adipocytes (Figures 1A–1E and Supplementary Table S1). Although absent in HFD-fed WT mice, *foz/foz* mice present a prominent steatosis as shown histologically (Figures 1F and 1G) and by a significant increase in liver weight (Supplementary Table S1). Lipid load in hepatic and adipose *foz/foz* tissues is associated with significant inflammation confirmed by increased expression of activated macrophages markers and of pro-inflammatory cytokines (Figures 1H and 1I). HFD causes insulin resistance in *foz/foz* but not in WT mice as assessed by increased fasting glucose and C-peptide levels (1409 ± 265 pM compared with 601 ± 98 pM; $P < 0.05$), decreased glucose lowering effect of insulin during insulin tolerance test (ITT) and increased glucose excursion curve and insulin secretion during glucose tolerance test (Figures 1J–1M).

WT-matched calorie intake is not sufficient to prevent obesity and glucose intolerance in HFD-fed *foz/foz* mice

To evaluate the contribution of increased food intake to the metabolic phenotype of *foz/foz* mice, we performed a pair-feeding experiment in which HFD intake in pair-fed *foz/foz* mice was restricted to exactly match that of WT mice (Figure 1A).

Although pair-feeding tends to reduce body weight gain and adipose tissue weight (Figures 1B and 1C), pair-fed *foz/foz* mice gain significantly more weight (Figure 1B), develop more adiposity (Figure 1C), have larger adipocytes (Figures 1D and 1E) and adipose inflammation (Figure 1I) than isocalorically HFD-fed WT mice. Pair-feeding in *foz/foz* mice ameliorates liver steatosis (Figures 1F and 1G) and decreases liver weight (Supplementary Table S1), normalizes fasting glucose (Figure 1J) and C-peptide levels (Figure 1M) and restores insulin sensitivity during insulin test to HFD-WT levels (Figure 1K). Although improved, glucose intolerance is not totally corrected by pair-feeding in *foz/foz* mice (Figure 1L).

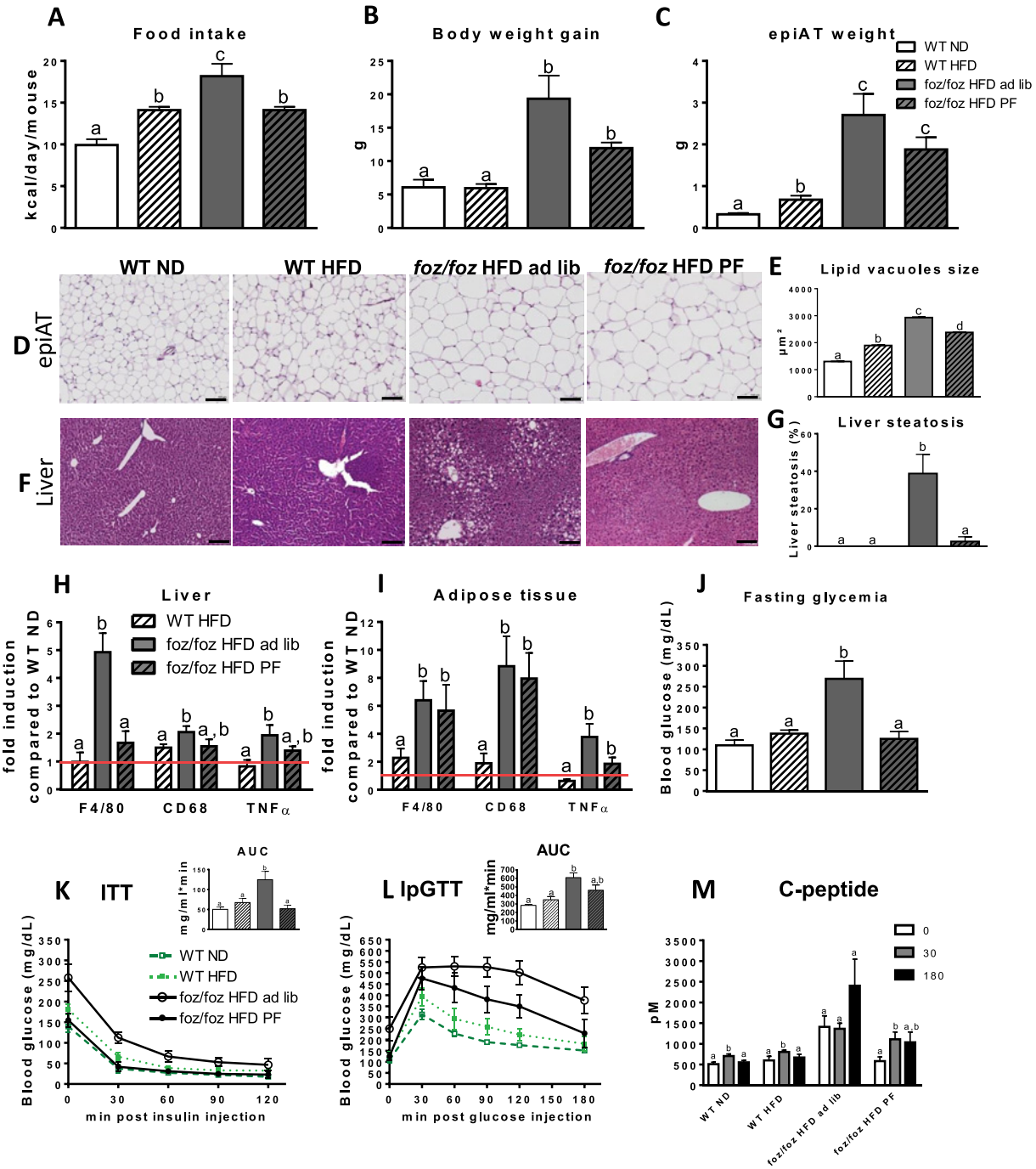

Figure 1 **Effects of caloric restriction to HFD-fed *foz/foz* mice for 4 weeks**

(**A**) Food intake, (**B**) body weight gain and (**C**) epididymal adipose tissue (epiAT) weight in WT fed a normal chow (ND), in WT and *foz/foz* mice fed a HFD *ad libitum* and in *foz/foz* mice pair-fed with WT mice under HFD (HFD PF) for 4 weeks. (**D** and **F**) Haematoxylin and eosin staining of epiAT and liver sections (scale bars = 100 μm). (**E**) Morphometrical assessment of lipid vacuoles size in epiAT in the different groups and (**G**) histological quantification of liver steatosis. Expression of inflammatory genes by RT-qPCR in (**H**) liver and (**I**) epiAT. Red lines indicate levels in WT control mice (WT ND). (**J**) Fasting blood glucose, glucose curves during intraperitoneal insulin (**K**) and glucose (**L**) tolerance test; AUC are presented in insets. (**M**) Plasmatic C-peptide level at 0, 30 or 180 min after glucose injection. Data are mean ± S.E.M. (n=5 per group). Data with different subscript letters are statistically different ($P < 0.05$).

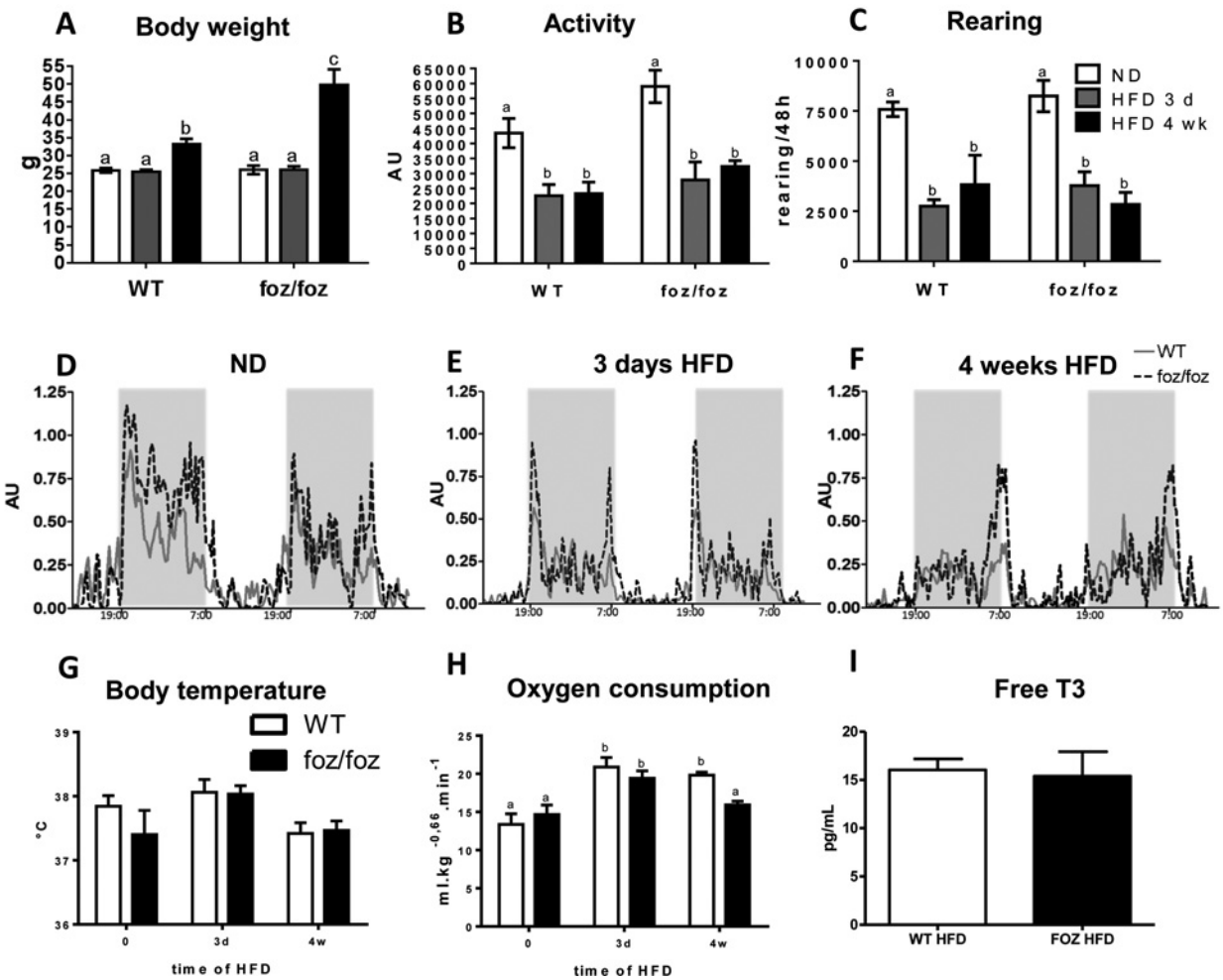

Figure 2 **Similar activity level pattern but decreased oxygen consumption in obese *foz/foz* mice compared with WT mice**

(**A**) Body weight, (**B**) horizontal activity and (**C**) vertical activity (rearing) were measured successively in WT and *foz/foz* mice 0, 3 and 28 days after HFD introduction in metabolic cages. (**D**–**F**) Similar circadian rhythm of activity between WT and *foz/foz* mice fed a ND or HFD. Body temperature (**G**) and oxygen consumption (**H**) in WT and *foz/foz* mice. (**I**) Plasmatic level of T3 in WT and *foz/foz* mice fed a HFD for 4 weeks. Data are represented as mean ± S.E.M. (n=6–10 per group). Data with different subscript letters are statistically different ($P < 0.05$).

These results demonstrate that hyperphagia contributes to liver steatosis, inflammation and fasting glycaemia but does not explain the obese phenotype of *foz/foz* mice.

Obese *foz/foz* mice have a similar physical activity level but a lower oxygen consumption compared with WT mice

To evaluate whether decreased muscle energy utilization participates in diabesity in *foz/foz* mice, we recorded 48 h physical activity repeatedly in mice on a chow diet and after 3 days and 4 weeks cumulative exposure to HFD. On chow, WT and *foz/foz* mice have similar spontaneous activity (Figures 2B and 2C) and similar patterns of nocturnal activity/diurnal rest (Figure 2D). HFD feeding similarly and drastically decreases the level of activity without disruption of the circadian pattern in both genotypes (Figures 2B–2F). Notably, the reduced activity in HFD-fed animals occurs prior to weight gain (Figure 2A).

Body temperature when on chow or on HFD (Figure 2G), resting oxygen consumption in chow-fed mice and increased oxygen consumption in response to HFD (Figure 2H) as well as plasma free T3 levels (Figure 2I) are similar in both genotypes. However, when *foz/foz* mice get obese, they reduce their oxygen consumption unlike WT mice. This collectively suggests that decreased energy utilization leading to the dysmetabolic phenotype of *foz/foz* mice is associated with decreased oxygen consumption but is not due to lower physical activity.

foz/foz mice have a defective HFD- and cold-induced non-shivering thermogenesis

We then evaluated the thermogenic capacity, a function chiefly located in the interscapular BAT in mice. When fed standard chow, *foz/foz* mice have a larger and fatter BAT (Figures 3A and 3B) than WT mice. Mitochondrial density is lower in ND-fed *foz/foz* mice (Figure 3E) but the level of expression of

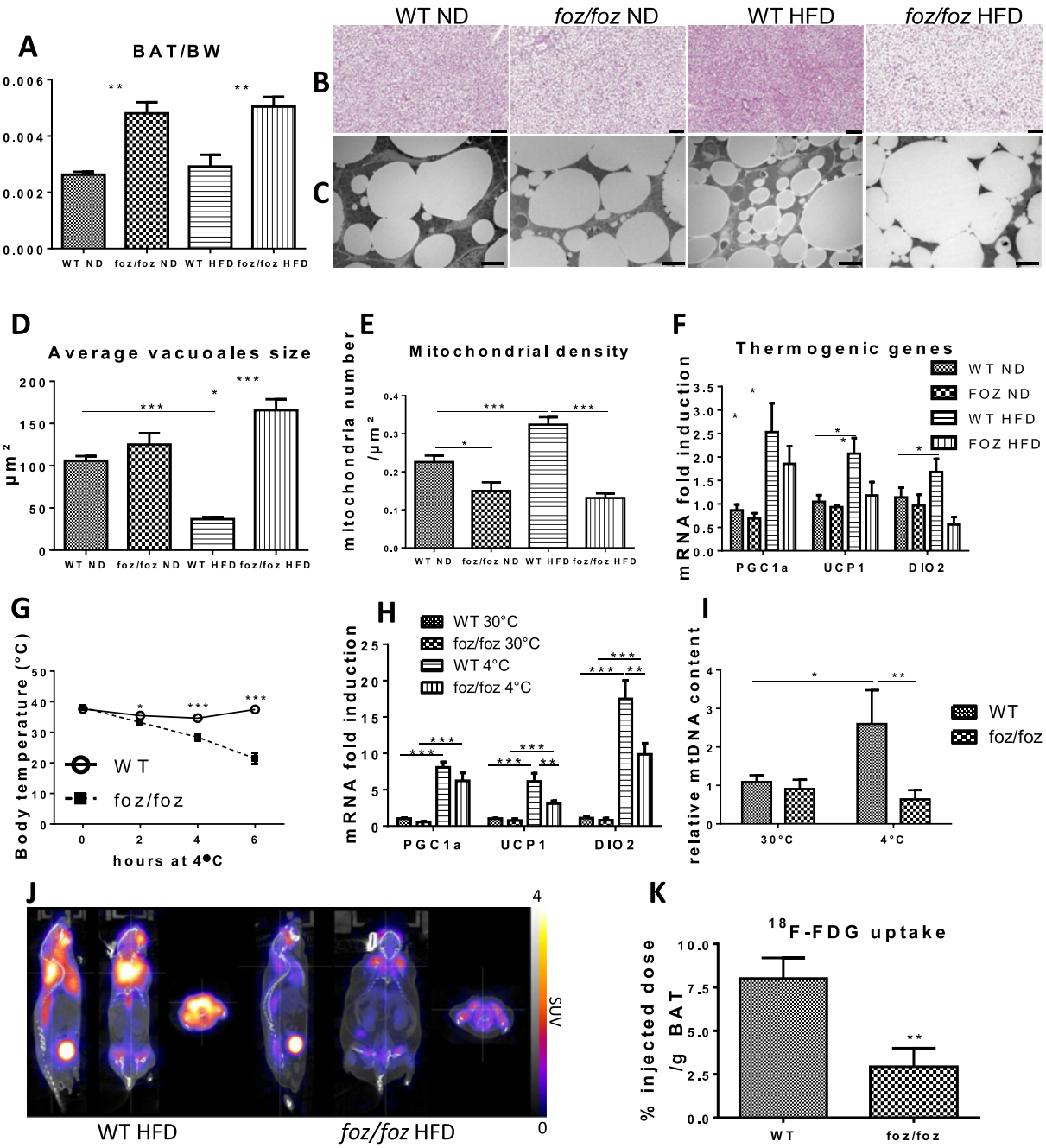

Figure 3 **Defective adaptive thermogenesis in response to HFD and acute cold exposure in *foz/foz* mice**

(**A**–**F**) WT and *foz/foz* mice were fed a HFD for 4 weeks and kept all the time at room temperature (22 °C). (A) BAT weight relative to body weight. (B) Haematoxylin and eosin staining (scale bars = 100 μm) and (C) representative EM images of BAT (scale bars = 50 nm). Morphometrical assessment of (D) average vacuoles size and (E) mitochondrial density in brown adipocytes. (F) mRNA expression of thermogenic genes (PGC1α, UCP1 and DIO2) in BAT. (**G**–**K**) WT and *foz/foz* mice were fed a HFD for 4 weeks, housed at thermoneutrality (30 °C) and exposed or not to 4 °C for 6 h before killing. (G) Body temperature of WT and *foz/foz* mice exposed for 6 h at 4 °C. (H) mRNA expression of thermogenic genes in BAT of WT and *foz/foz* mice culled at thermoneutrality or after 6 h at 4 °C. (I) mtDNA content in BAT as the ratio of mitochondrial COXII to nuclear β-2-microglobulin DNA determined by RT-qPCR. (J) PET/CT sagittal, coronal and axial images 1 h after injection of ^{18}F-FDG in WT and *foz/foz* mice exposed to 4 °C for 4 h. PET images were normalized to SUVmax of 4. (K) Percentage of ^{18}F-FDG injected dose per gram of BAT. Data are represented as mean ± S.E.M. (n=6 per group); $*P < 0.05$, $**P < 0.01$, $***P < 0.001$.

thermogenic genes UCP-1, peroxisome proliferator-activated receptor γ co-activator 1 α (PGC1α) and type II iodothyronine deiodinase (DIO2) is similar between the two genotypes (Figure 3F). When WT mice are fed the HFD, we observed a decrease in the size of lipid vacuoles (Figure 3D), an increased BAT mitochondrial density (Figure 3E) and an up-regulation of genes implicated in thermogenesis (Figure 3F). Conversely, in *foz/foz* mice, HFD feeding leads to a marked increase in lipid load in BAT (Figure 3B and Supplementary Figure S2) that exhibits larger lipid vacuoles (Figure 3D). BAT mitochondrial density remains unchanged (Figure 3E) and up-regulation of thermogenic genes in response to HFD is lower (PGC1α or UCP1) or blunted (DIO2) compared with the response of WT mice (Figure 3F). The results support that, in contradistinction to WT mice, *foz/foz* mice have a defective HFD-induced thermogenic capacity.

To evaluate thermogenic adaptation to cold temperature, mice were housed at thermoneutrality (30 °C), fed a HFD for 4 weeks and then exposed to 4 °C for 6 h. During cold exposure, body temperature barely changes (−0.3 °C) in WT mice but critically drops to 16.7 °C in *foz/foz* mice (Figure 3G). Cold intolerance observed in *foz/foz* mice was not associated with reduced shivering, an effective short-term thermogenic mechanism, and therefore suggests a deficient BAT function (Supplementary Figure S1). The expression of thermogenic genes is largely up-regulated in both WT and *foz/foz* mice (Figure 3H) but cold-induction of UCP1 and DIO2 is significantly lower in HFD-fed *foz/foz* than in HFD-fed WT mice (Figure 3H). Moreover, BAT mtDNA increases only in WT but not in *foz/foz* mice (Figure 3I). A PET/CT was performed to assess BAT function *in vivo*: the BAT uptake of ^{18}F-FDG upon cold exposure was significantly lower in *foz/foz* than in WT mice (Figures 3J and 3K). All these results demonstrate a failure of adaptive thermogenesis in *foz/foz* mice.

BAT adrenergic pathway is impaired in *foz/foz* mice

The sympathetic nervous system is the most important regulator of BAT function [8]. At thermoneutrality, BAT NE content is lower in *foz/foz* than in WT BAT (Figure 4B) and upon cold exposure, the levels of dopamine, NE and adrenaline are lower in *foz/foz* than in WT BAT (Figures 4A–4C). In keeping, lower tyrosine hydroxylase content demonstrated by fluorescent immunohistochemistry supports lower *in situ* catecholamine production in *foz/foz* BAT (Figures 4D and 4E). In addition to a decreased sympathetic innervation, sympathetic activity was also reduced in BAT of *foz/foz* mice upon cold exposure, as assessed by a decreased NE turnover in their BAT (Figure 4F). At thermoneutrality as well as after cold stimulation, the expression of β3-adrenergic receptor (β3AR), the most abundant adrenergic receptor in BAT [21], is lower in *foz/foz* compared with WT BAT (Figure 4G). Conversely, expression of β2AR, a minor isoform, is strongly up-regulated by cold in *foz/foz* but not in WT BAT. Consistent with decreased adrenergic tone, cAMP, the second messenger of the adrenergic pathway, is also lower at thermoneutrality (ANOVA $P = 0.05$ for genotype) and is not induced upon cold exposure in *foz/foz,* unlike in WT BAT (Figure 4H). Bone morphogenetic protein 8B (BMP8B), a molecule that increases the adrenergic sensitivity of mature brown adipocytes [22], is significantly induced upon cold exposure in WT but not in *foz/foz* BAT (Figure 4I). These results support that decreased β-adrenergic signalling contributes to adaptive failure of the BAT in *foz/foz* mice.

Repeated cold exposure improves thermogenic function in BAT and the phenotype of *foz/foz* mice

We reasoned that repeated stimulation of the sympathetic axis may cause sufficient activation of the thermogenic pathway to prevent *foz/foz* phenotype. We thus performed an ICE experiment in which HFD-fed WT and *foz/foz* mice were exposed to 4 °C ambient temperature for two consecutive hours a day during 4 weeks and compared with their littermates housed at all times at 22 °C. Compared with "unchallenged" *foz/foz* mice, *foz/foz* mice under ICE protocol present (i) a decreased BAT fat content (Figure 5A and Table 1); (ii) a remarkable maintenance of body temperature after 6 h at 4 °C similar to that of WT mice (Figure 5C) whereas in "unchallenged" *foz/foz* mice, body temperature critically falls under 20 °C in the same conditions of cold exposure (Figure 3G); (iii) an increased tyrosine hydroxylase content (Figure 5D); (iv) an up-regulation of BMP8B mRNA level (Figure 5G); (v) an increased level of dopamine in BAT similar to that of WT mice (Figure 5E) and (vi) an up-regulation of thermogenic (PGC1α, UCP1 and DIO2) and lipolytic [peroxisome proliferator-activated receptor α (PPARα) and cluster of differentiation 36 (CD36)] genes in BAT similar to that of WT mice (here again, not seen in mice that were not repeatedly exposed to cold – Figure 3H) (Figure 5G).

In the inguinal white adipose tissue (ingWAT), ICE protocol in *foz/foz* mice reduces adipocyte size, induces UCP-1 positive brown-like adipocytes (Figure 5B and Table 1), induces the expression of UCP1 and lipid β-oxidation gene acyl CoA oxidase (ACOX) (Figure 5H) and enhances sympathetic innervation (not shown) to a similar extent as in WT mice.

Remarkably, although food intake is similar, the better thermogenic function in ICE *foz/foz* mice is associated with a reduced body weight gain and fat load in white adipose depots (Figure 5I and Table 1). It reduces fasting blood glucose (Figure 5J) and significantly improves glucose tolerance in *foz/foz* mice (Figure 5K and Table 1). Moreover, ICE in *foz/foz* mice is associated with a reduced liver weight (Figure 5L) and steatosis (Figure 5M and Table 1). Thus, ICE rescues thermogenic function in BAT and enables browning of white adipose in *foz/foz* mice through an increase of the sympathetic tone. This leads to an improvement of *foz/foz* phenotype.

DISCUSSION

In the present study, we identified, next to hyperphagia, altered BAT function as a significant contributor to obesity, glucose intolerance and liver steatosis in *foz/foz* mice in response to HFD. In WT mice, HFD induces a thermogenic activity as an adaptive process to counteract energy overload. This is evidenced by increased BAT mitochondrial content, β-oxidation and uncoupling gene expression. Conversely, this physiological response is not seen in HFD-fed *foz/foz* mice. Failure of adaptive BAT thermogenic response in *foz/foz* mice was even better

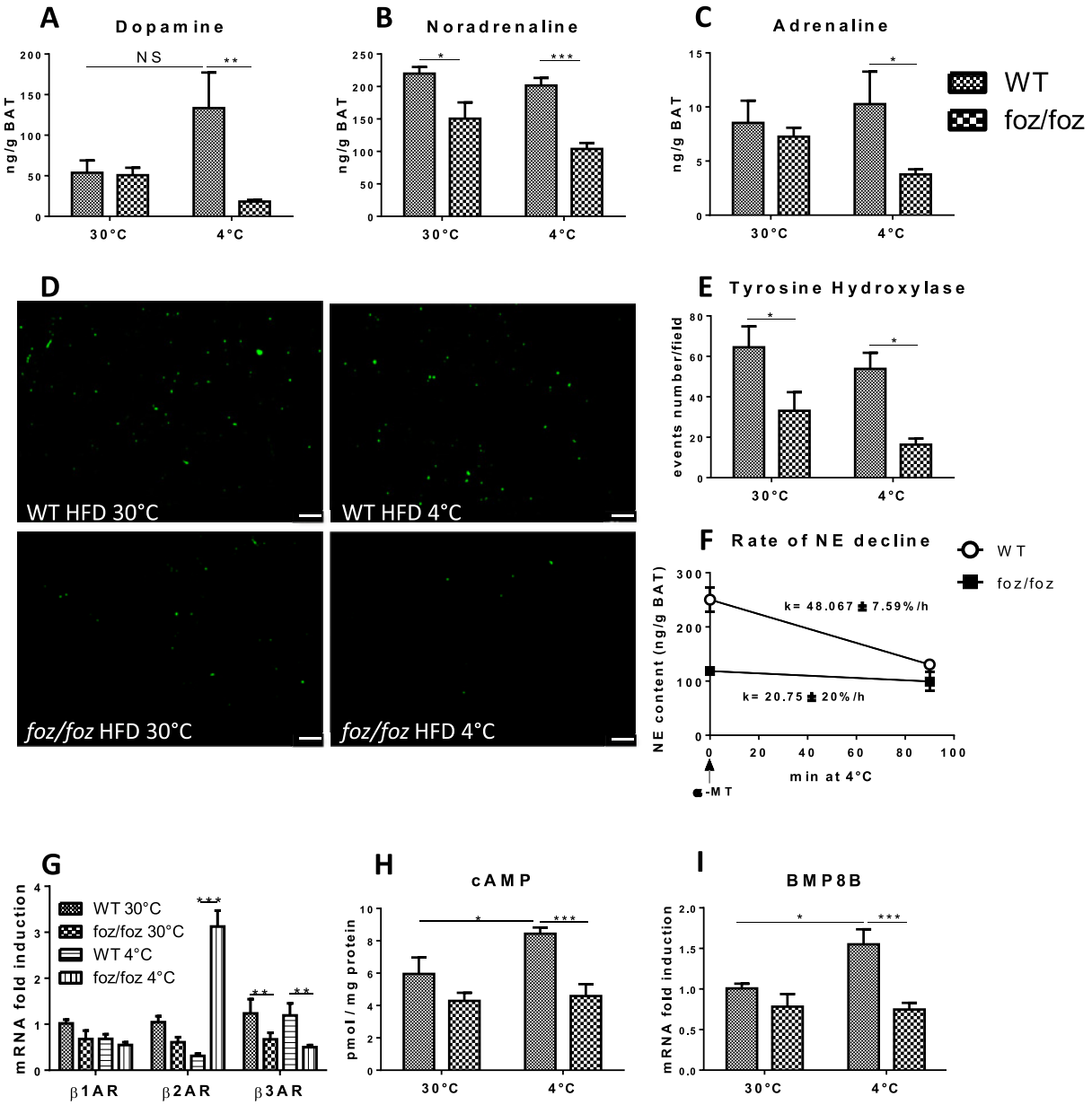

Figure 4 **Impaired adrenergic signalling in BAT of *foz/foz* mice**

WT and *foz/foz* mice were fed a HFD for 4 weeks, kept at thermoneutrality and then exposed or not to 4 °C for 6 h before killing. (**A**) Level of dopamine, (**B**) NE and (**C**) adrenaline in BAT. (**D**) Immunofluorescence staining of tyrosine hydroxylase (scale bar = 50 μm) and (**E**) quantification of (D). (**F**) Rate of NE decline in BAT. (**G**) mRNA expression of βARs in BAT in the different groups. (**H**) cAMP level in BAT. (**I**) mRNA expression of BMP8B in BAT. Data are represented as mean ± S.E.M. (n=6 per group); $*P < 0.05$, $**P < 0.01$, $***P < 0.001$.

exemplified when animals were exposed to cold temperatures. Indeed, when the temperature of the environment dropped to 4 °C, metabolic activation in the BAT was insufficient to maintain a body temperature compatible with survival in HFD-fed *foz/foz* mice.

We were surprised to see that reduced physical activity did not contribute to the obese phenotype of *foz/foz* mice. Even more surprising was that HFD so rapidly decreased spontaneous activity in both WT and *foz/foz* mice, well before the onset of obesity. The literature provides little and conflicting data pertaining to this: some reports suggest that the relative increase in saturated fat compared with unsaturated fat matters [23–25] whereas other suggest a contribution of HFD-induced insulin resistance [23] or secondary obesity. In the model we used, we propose that the addition of high saturated lipid intake and decreased muscle energy expenditure results in to rapid obesity and insulin resistance if not compensated for by brown adipose energy combustion.

To confirm this, we sought experimental modulation of BAT function. Indeed, repeated cold exposure (ICE experiment) that successfully stimulates BAT activity in HFD-fed *foz/foz* mice,

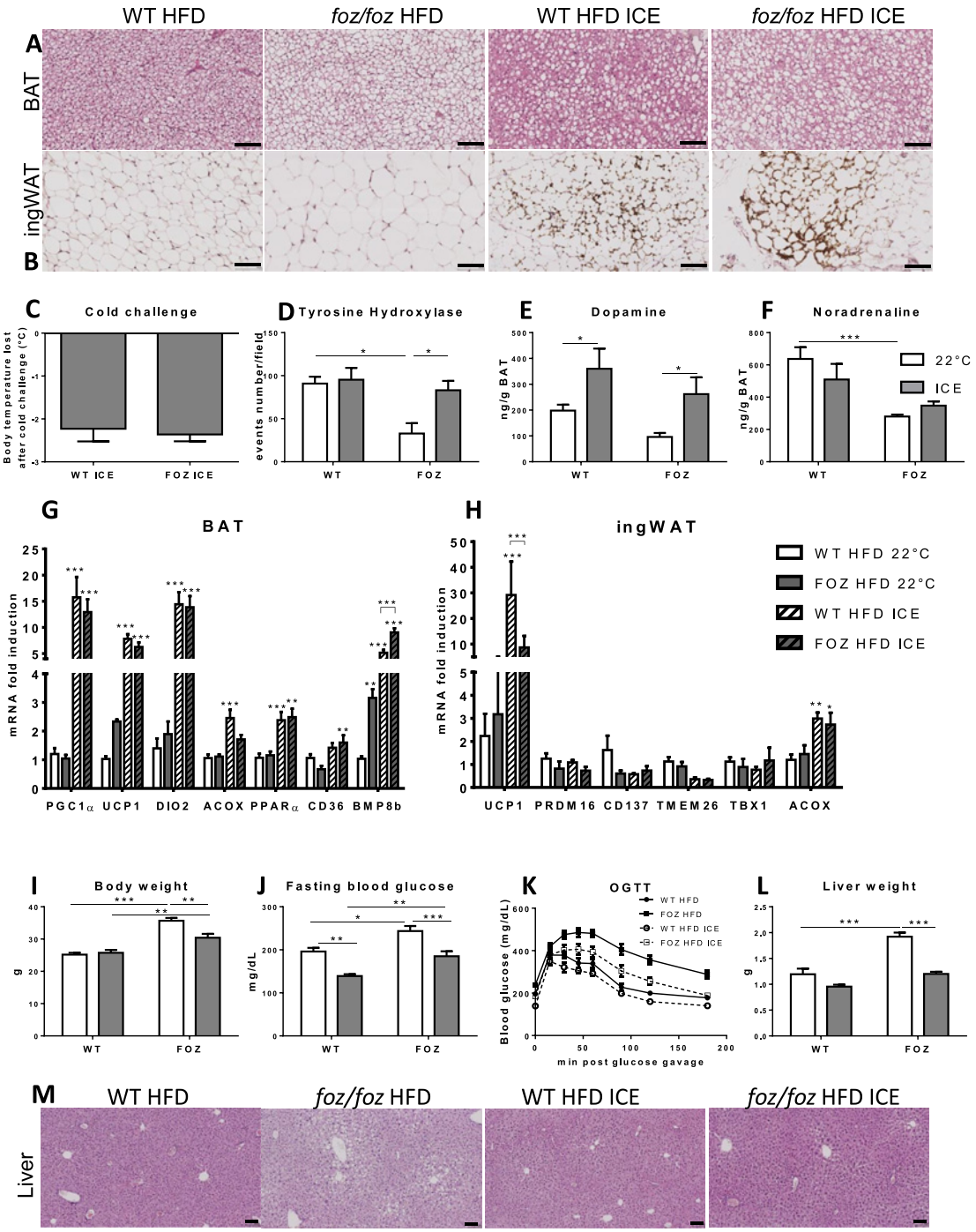

Figure 5 **ICE increased thermogenic capacities in BAT and WAT leading to an improvement of *foz/foz* phenotype**

WT and *foz/foz* mice were exposed to 4 °C ambient temperature for two consecutive hours a day during 4 weeks (ICE) and compared with their littermates housed at all times at 22 °C. (**A**) Haematoxylin and eosin staining of BAT and (**B**) immunohistochemical staining of UCP1 in ingWAT. (**C**) Body temperature measured before and after 6 h at 4 °C in WT and *foz/foz* ICE mice. (**D**) Quantification of tyrosine hydroxylase staining in BAT. (**E**) Level of dopamine and (**F**) NE in BAT. mRNA expression of genes involved in thermogenesis, β-oxidation and adrenergic sensitization (**G**) in BAT and (**H**) in ingWAT. (**I**) Body weight at the end of the experiment. (**J**) Fasting blood glucose and (**K**) glucose tolerance test 3 weeks after the beginning of the experiment. (**L**) Liver weight and (**M**) haematoxylin and eosin staining of liver sections (bar size, 100 μm). Data are represented as mean $\pm$ S.E.M. (n=8 per group); $^*P < 0.05$, $^{**}P < 0.01$, $^{***}P < 0.001$.

Table 1 Effects of ICE on food intake, body and tissues weight and lipid content in HFD-fed WT and *foz/foz* mice and glucose homoeostasis

	WT HFD	*foz/foz* HFD	WT HFD ICE	*foz/foz* HFD ICE
Food intake (g HFD/day per mouse)	2.49 ± 0.15^{A}	2.96 ± 0.44^{B}	2.45 ± 0.27^{A}	2.72 ± 0.25^{AB}
Body weight gain (g)	4.69 ± 2.48^{A}	15.63 ± 3.05^{B}	4.53 ± 1.28^{A}	11.00 ± 2.92^{C}
epiAT weight (g)	0.65 ± 0.31^{A}	2.02 ± 0.27^{B}	0.86 ± 0.20^{A}	1.55 ± 0.70^{C}
ingWAT weight (g)	0.32 ± 0.16^{A}	1.55 ± 0.69^{B}	0.47 ± 0.09^{A}	0.64 ± 0.22^{A}
BAT weight (g)	0.10 ± 0.03^{A}	0.19 ± 0.04^{B}	0.11 ± 0.04^{A}	0.18 ± 0.09^{B}
BAT lipid content (%)	46.65 ± 12.0^{A}	63.54 ± 6.92^{B}	37.31 ± 7.78^{A}	48.15 ± 7.52^{A}
Inguinal adipocytes size (μm^2)	1525 ± 632^{A}	3389 ± 759^{B}	1492 ± 198^{A}	2241 ± 445^{A}
Liver steatosis (%)	0.00 ± 0.0^{A}	39.1 ± 20.6^{B}	4.28 ± 11.3^{A}	13.57 ± 12.5^{C}
OGTT (AUC) [(mg/dl) $\times$ 180 min]	46752 ± 6570^{A}	70185 ± 12195^{B}	39649 ± 3092^{A}	54367 ± 10924^{C}

Data are expressed as mean $\pm$ S.D. Two-way ANOVA followed by post-hoc Bonferroni's analysis. Different letters identify significant differences between groups ($P < 0.05$).

minimizes the body weight gain and glucose intolerance. This improvement occurred without changes in food intake. We also established a positive correlation between increased thermogenic capacity and decreased liver steatosis. In support of other animal studies [9,26,27], our study provides experimental evidence of the therapeutic potential of BAT stimulation for metabolic syndrome and its hepatic complication.

Our data support that failure of adaptive thermogenesis in *foz/foz* mice is due to a defective sympathetic signalling as shown by lower sympathetic innervation and activity, β3AR expression, catecholamine and cAMP content in their BAT. Whether this is a primary or a secondary event in *foz/foz* mice is unclear. Evidence against a primary defect due to ALMS1 mutation are that the thermogenic response is operating in young ND-fed *foz/foz* mice, that the sympathetic hypotonus is reversed by ICE and that low sympathetic activity particularly in BAT, is also present in other genetic model of severe obesity [21,28,29]. Also, low sympathetic nervous system activity is proposed as a risk factor for obesity in humans [30] and leptin, to which obese humans and mice are resistant, has been shown to increase NE turnover and sympathetic innervation in thermogenic BAT [31]. We suggest that ALMS1 mutation predisposes to energy overload, in particular in BAT, causing a secondary adrenergic defect. Much more experimental work will be needed to address the mechanisms involved.

Altogether, defective BAT adaptation in *foz/foz* mice significantly contributes to obesity, glucose intolerance and fatty liver. Restitution of BAT activity enables homoeostatic energy expenditure through thermogenesis and improves obesity and dysmetabolic complications. Noteworthy, physiological BAT function protects the liver and prevents steatosis. BAT function must thus be seen as one of the multiple-hits leading to NAFLD pathogenesis in the context of obesity.

Functional studies confirmed that residual BAT is present in human adults [32,33] and have established that the tissue could contribute to 3–5% of the basal metabolic rate [34]. Increased BAT stimulation has also a positive effect on energy expenditure in healthy patients [35]. Hanssen et al. [36] showed that 10-day cold acclimation in obese Type 2 diabetes patients could increase BAT activity and peripheral insulin sensitivity. Another study reported a 13% increase in basal metabolic rate in healthy subjects as a result of BAT activation upon an acute administration of mirabegron, a β3AR agonist [37]. No data are available regarding metabolic improvement upon β3AR agonist treatment and it remains uncertain if chronic and systemic β3AR-mediated stimulation of BAT is possible without encountering the cardiovascular side effects often associated with β adrenergic receptor (βAR) agonists.

In summary, BAT's failure to adapt to dietary energy overload, through a mechanism involving impaired sympathetic tone, partly contributes to obesity, metabolic syndrome and liver complications in *foz/foz* mice. Repeated cold exposure, by restoring the sympathetic tone, stimulates thermogenic function (via activation of both brown adipocyte and browning in WAT) and prevents obesity, metabolic syndrome and NAFLD development. The present study provides hope for the success of BAT stimulation therapy for human obesity syndrome and its hepatic complications.

CLINICAL PERSPECTIVES

- NAFLD pathogenesis is not fully understood and effective therapeutics are not available.
- In the present study, we identified defective adaptive thermogenesis as a contribution factor to metabolic syndrome and NAFLD development.
- Targeting BAT represents a potential strategy for the management of metabolic syndrome and its hepatic complications.

AUTHOR CONTRIBUTION

Laurence Poekes and Isabelle Leclercq designed research; Laurence Poekes performed research; Anne Bol and Olivier Schakman contributed analytic tools; Christine Detrembleur provided the experimental platform, technical and scientific assistance for measuring shivering; Laurence Poekes and Isabelle Leclercq wrote the paper; Vanessa Legry, Yves Horsmans and Geoffrey Farrell revised the paper critically. Laurence Poekes and Isabelle Leclercq are the guarantors of this work and, as such, had full access to all the data in the study and take responsibility for the integrity of the data and the accuracy of the data analysis.

ACKNOWLEDGEMENTS

We thank Natacha Feza-Bingi (Bouzin UCL, Brussels, Belgium) and Mathilde Beka (UCL, Brussels, Belgium) for animal breeding, genotyping and care, and Caroline Bouzin (UCL, Brussels, Belgium) for the histological quantification setup. We also thank Professor J.L. Balligand and Professor Chantal Dessy (UCL, Brussesl, Belgium) for scientific discussion pertaining to assessment of the sympathetic pathway.

FUNDING

This work was supported by the Communauté française de Belgique – Actions de Recherche Concertées [grant number 12/17-047]; the Fund for Scientific Medical Research [grant number PDR T.1067.14] and unrestricted research grants from Gilead Belgium, Janssens Pharmaceutica Belgium, and Roche Belgium. I.A.L. is senior research associate with the Belgian National Fund for Scientific Research (FNRS) and fellowship to V.L. has been supported by the Institut de Recherche expérimentale et Clinique (IREC) at the Université catholique de Louvain, Brussels, Belgium. The behavior platform was supported by the Programme d'Excellence Marshall, Wallonia regio and Université catholique de Louvain (Diane convention).

REFERENCES

1 Prentice, A.M. (2006) The emerging epidemic of obesity in developing countries. Int. J. Epidemiol. **35**, 93–99 CrossRef
2 World-Health-Organization (2015), Obesity and overweight (http://www.who.int/mediacentre/factsheets/fs311/en/)
3 de Ferranti, S., Mozaffarian, D. (2008) The perfect storm: obesity, adipocyte dysfunction, and metabolic consequences. Clin. Chem. **54**, 945–955 CrossRef
4 Bray, G.A., Fruhbeck, G., Ryan, D.H. and Wilding, J.P. (2016) Management of obesity. Lancet **387**, 1947–1956
5 Thomas, E.L., Brynes, A.E., Hamilton, G., Patel, N., Spong, A., Goldin, R.D., Frost, G., Bell, J.D. and Taylor-Robinson, S.D. (2006) Effect of nutritional counselling on hepatic, muscle and adipose tissue fat content and distribution in non-alcoholic fatty liver disease. World J. Gastroenterol. **12**, 5813–5819 CrossRef
6 Huang, M.A., Greenson, J.K., Chao, C., Anderson, L., Peterman, D., Jacobson, J., Emick, D., Lok, A.S. and Conjeevaram, H.S. (2005) One-year intense nutritional counseling results in histological improvement in patients with non-alcoholic steatohepatitis: a pilot study. Am. J. Gastroenterol. **100**, 1072–1081 CrossRef
7 Poekes, L., Lanthier, N. and Leclercq, I.A. (2015) Brown adipose tissue: a potential target in the fight against obesity and the metabolic syndrome. Clin. Sci. **129**, 933–949 CrossRef
8 Cannon, B. and Nedergaard, J. (2004) Brown adipose tissue: function and physiological significance. Physiol. Rev. **84**, 277–359 CrossRef
9 Hamann, A., Flier, J.S. and Lowell, B.B. (1998) Obesity after genetic ablation of brown adipose tissue. Zeitschrift fur Ernahrungswissenschaft **37** (Suppl 1), 1–7
10 Vijgen, G.H., Bouvy, N.D., Teule, G.J., Brans, B., Schrauwen, P. and van Marken Lichtenbelt, W.D. (2011) Brown adipose tissue in morbidly obese subjects. PloS One **6**, e17247 CrossRef
11 Larter, C.Z. and Yeh, M.M. (2008) Animal models of NASH: getting both pathology and metabolic context right. J. Gastroenterol. Hepatol. **23**, 1635–1648 CrossRef
12 Arsov, T., Larter, C.Z., Nolan, C.J., Petrovsky, N., Goodnow, C.C., Teoh, N.C., Yeh, M.M. and Farrell, G.C. (2006) Adaptive failure to high-fat diet characterizes steatohepatitis in Alms1 mutant mice. Biochem. Biophys. Res. Commun. **342**, 1152–1159 CrossRef
13 Arsov, T., Silva, D.G., O'Bryan, M.K., Sainsbury, A., Lee, N.J., Kennedy, C., Manji, S.S., Nelms, K., Liu, C., Vinuesa, C.G. et al. (2006) Fat aussie – a new Alstrom syndrome mouse showing a critical role for ALMS1 in obesity, diabetes, and spermatogenesis. Mol. Endocrinol. **20**, 1610–1622 CrossRef
14 Larter, C.Z., Yeh, M.M., Van Rooyen, D.M., Teoh, N.C., Brooling, J., Hou, J.Y., Williams, J., Clyne, M., Nolan, C.J. and Farrell, G.C. (2009) Roles of adipose restriction and metabolic factors in progression of steatosis to steatohepatitis in obese, diabetic mice. J. Gastroenterol. Hepatol. **24**, 1658–1668 CrossRef
15 Legry, V., Van Rooyen, D.M., Lambert, B., Sempoux, C., Poekes, L., Espanol-Suner, R., Molendi-Coste, O., Horsmans, Y., Farrell, G.C. and Leclercq, I.A. (2014) Endoplasmic reticulum stress does not contribute to steatohepatitis in obese and insulin-resistant high-fat-diet-fed foz/foz mice. Clin. Sci. **127**, 507–518 CrossRef
16 Gathercole, L.L., Hazlehurst, J.M., Armstrong, M.J., Crowley, R., Boocock, S., O'Reilly, M.W., Round, M., Brown, R., Bolton, S., Cramb, R. et al. (2016) Advanced non-alcoholic fatty liver disease and adipose tissue fibrosis in patients with Alstrom syndrome. Liver Int. **36**, 1704–1712 CrossRef
17 Heydet, D., Chen, L.X., Larter, C.Z., Inglis, C., Silverman, M.A., Farrell, G.C. and Leroux, M.R. (2013) A truncating mutation of Alms1 reduces the number of hypothalamic neuronal cilia in obese mice. Dev. Neurobiol. **73**, 1–13 CrossRef
18 Dombret, C., Nguyen, T., Schakman, O., Michaud, J.L., Hardin-Pouzet, H., Bertrand, M.J. and De Backer, O. (2012) Loss of Maged1 results in obesity, deficits of social interactions, impaired sexual behavior and severe alteration of mature oxytocin production in the hypothalamus. Hum. Mol. Genet. **21**, 4703–4717 CrossRef
19 White, C.R. and Seymour, R.S. (2003) Mammalian basal metabolic rate is proportional to body mass2/3. Proc. Natl. Acad. Sci. U.S.A. **100**, 4046–4049 CrossRef
20 Spector, S., Sjoerdsma, A. and Udenfriend, S. (1965) Blockade of endogenous norepinephrine synthesis by alpha-methyl-tyrosine, an Inhibitor of tyrosine hydroxylase. J. Pharmacol. Exp. Ther. **147**, 86–95
21 Collins, S., Daniel, K.W., Rohlfs, E.M., Ramkumar, V., Taylor, I.L. and Gettys, T.W. (1994) Impaired expression and functional activity of the beta 3- and beta 1-adrenergic receptors in adipose tissue of congenitally obese (C57BL/6J ob/ob) mice. Mol. Endocrinol. **8**, 518–527
22 Whittle, A.J., Carobbio, S., Martins, L., Slawik, M., Hondares, E., Vazquez, M.J., Morgan, D., Csikasz, R.I., Gallego, R., Rodriguez-Cuenca, S. et al. (2012) BMP8B increases brown adipose tissue thermogenesis through both central and peripheral actions. Cell **149**, 871–885 CrossRef
23 Ramadan, W., Dewasmes, G., Petitjean, M., Loos, N., Delanaud, S., Geloen, A. and Libert, J.P. (2006) Spontaneous motor activity in fat-fed, streptozotocin-treated rats: a nonobese model of type 2 diabetes. Physiol. Behav. **87**, 765–772 CrossRef
24 Kameyama, T., Ohhara, T., Nakashima, Y., Naito, Y., Huang, M.Z., Watanabe, S., Kobayashi, T., Okuyama, H., Yamada, K. and Nabeshima, T. (1996) Effects of dietary vegetable oils on behavior and drug responses in mice. Biol. Pharm. Bull. **19**, 400–404 CrossRef
25 Wong, C.K., Botta, A., Pither, J., Dai, C., Gibson, W.T. and Ghosh, S. (2015) A high-fat diet rich in corn oil reduces spontaneous locomotor activity and induces insulin resistance in mice. J. Nutr. Biochem. **26**, 319–326 CrossRef
26 Stanford, K.I., Middelbeek, R.J., Townsend, K.L., An, D., Nygaard, E.B., Hitchcox, K.M., Markan, K.R., Nakano, K., Hirshman, M.F., Tseng, Y.H. and Goodyear, L.J. (2013) Brown adipose tissue regulates glucose homeostasis and insulin sensitivity. J. Clin. Investig. **123**, 215–223 CrossRef

27 Bartelt, A., Bruns, O.T., Reimer, R., Hohenberg, H., Ittrich, H., Peldschus, K., Kaul, M.G., Tromsdorf, U.I., Weller, H., Waurisch, C. et al. (2011) Brown adipose tissue activity controls triglyceride clearance. Nat. Med. **17**, 200–205 CrossRef
28 Roseberry, A.G., Painter, T., Mark, G.P. and Williams, J.T. (2007) Decreased vesicular somatodendritic dopamine stores in leptin-deficient mice. J. Neurosci. **27**, 7021–7027 CrossRef
29 Young, J.B. and Landsberg, L. (1983) Diminished sympathetic nervous system activity in genetically obese (ob/ob) mouse. Am. J. Physiol. **245**, E148–E154
30 Ravussin, E. and Tataranni, P.A. (1996) The role of altered sympathetic nervous system activity in the pathogenesis of obesity. Proc. Nutr. Soc. **55**, 793–802 CrossRef
31 Collins, S., Kuhn, C.M., Petro, A.E., Swick, A.G., Chrunyk, B.A. and Surwit, R.S. (1996) Role of leptin in fat regulation. Nature **380**, 677 CrossRef
32 Saito, M., Okamatsu-Ogura, Y., Matsushita, M., Watanabe, K., Yoneshiro, T., Nio-Kobayashi, J., Iwanaga, T., Miyagawa, M., Kameya, T., Nakada, K. et al. (2009) High incidence of metabolically active brown adipose tissue in healthy adult humans: effects of cold exposure and adiposity. Diabetes **58**, 1526–1531 CrossRef
33 Cypess, A.M., Lehman, S., Williams, G., Tal, I., Rodman, D., Goldfine, A.B., Kuo, F.C., Palmer, E.L., Tseng, Y.H., Doria, A. et al. (2009) Identification and importance of brown adipose tissue in adult humans. N. Engl. J. Med. **360**, 1509–1517 CrossRef
34 van Marken Lichtenbelt, W.D. and Schrauwen, P. (2011) Implications of nonshivering thermogenesis for energy balance regulation in humans. Am. J. Physiol. Regul. Integr. Comp. Physiol. **301**, R285–R296 CrossRef
35 Yoneshiro, T., Aita, S., Matsushita, M., Kayahara, T., Kameya, T., Kawai, Y., Iwanaga, T. and Saito, M. (2013) Recruited brown adipose tissue as an antiobesity agent in humans. J. Clin. Invest. **123**, 3404–3408 CrossRef
36 Hanssen, M.J., Hoeks, J., Brans, B., van der Lans, A.A., Schaart, G., van den Driessche, J.J., Jörgensen, J.A., Boekschoten, M.V., Hesselink, M.K., Havekes, B. et al. (2015) Short-term cold acclimation improves insulin sensitivity in patients with type 2 diabetes mellitus. Nat. Med. **21**, 863–865 CrossRef
37 Cypess, A.M., Weiner, L.S., Roberts-Toler, C., Franquet Elia, E., Kessler, S.H., Kahn, P.A., English, J., Chatman, K., Trauger, S.A., Doria, A. and Kolodny, G.M. (2015) Activation of human brown adipose tissue by a beta3-adrenergic receptor agonist. Cell Metab. **21**, 33–38 CrossRef

Received 23 June 2016/31 October 2016; accepted 1 November 2016
Accepted Manuscript online 1 November 2016, doi: 10.1042/CS20160469

